

ON THE PROPER ORTHOGONAL MODES OF CONTINUOUS VIBRATION SYSTEMS

B. F. Feeny

Department of Mechanical Engineering
Michigan State University
East Lansing, MI 48824

Abstract

We investigate the interpretation of proper orthogonal modes (POMs) of displacements in both linear and nonlinear one-dimensional distributed-parameter vibration systems for which a discrete set of displacements are sampled, and the discretization is uniform. The POMs in undamped linear self-adjoint systems can approximately represent linear natural modes if the mass distribution is known. If a single mode dominates, the dominant POM approximates the dominant mode. This is also true of a distributed system of unknown mass that is discretized arbitrarily. For synchronous nonlinear normal modes, the dominant POM represents a best fit of the nonlinear modal curve. Linear and nonlinear simulation examples are presented.

Keywords: proper orthogonal decomposition, proper orthogonal modes, Karhunen-Loève decomposition, modal analysis, nonlinear normal modes.

1 INTRODUCTION

Proper orthogonal decomposition (POD), also known as Karhunen-Loève decomposition, has emerged as a useful experimental tool in dynamics and vibration. Lumley (1970) traced the idea back to independent investigations by Kosambi in 1943, Loève in 1945, Karhunen in 1946, Pougachev in 1953, and Obukhov in 1954. It is primarily a statistical formulation, although it facilitates modal projections of partial differential equations into reduced-order

deterministic models. The discrete formulation resembles singular value decomposition. A more thorough history of POD in this context is presented by Ravindra (1999).

The method was applied to turbulence by Lumley (1967), and recently has received considerable attention from structural dynamicists. A common application of POD to structures typically involves the sensed displacements, $x_1(t), x_2(t), \dots, x_M(t)$, at M locations on the structure. (The method is also amenable to sensed velocities (Giorgiou and Schwartz, 1996; Kreuzer and Kust, 1996).) When the displacements are sampled N times, we can form displacement-history arrays, such that $\mathbf{x}_i = (x_i(t_1), x_i(t_2), \dots, x_i(t_N))^T$, for $i = 1, \dots, M$. The mean values are often subtracted from the displacement histories. In performing the proper orthogonal decomposition, these displacement histories are used to form an $N \times M$ ensemble matrix,

$$\mathbf{X} = [\mathbf{x}_1, \mathbf{x}_2, \dots, \mathbf{x}_M].$$

Each row of \mathbf{X} represents a point in the coordinate space at a particular instant in time. The $M \times M$ correlation matrix $\mathbf{R} = \frac{1}{N} \mathbf{X}^T \mathbf{X}$ is then formed. Since \mathbf{R} is real and symmetric, its eigenvectors form an orthogonal basis. The eigenvectors of \mathbf{R} are the proper orthogonal modes (POMs), and the eigenvalues are the proper orthogonal values (POVs). In the analysis of turbulence, the POMs have been shown to represent the optimal distributions of kinetic energy or power, and the proper orthogonal values (POVs) indicate the power associated with these principal distributions (Berkooz *et al.*, 1993; Cusumano *et al.*, 1993). Alternatively, the POMs represent the principal axes of inertia of the data in the measurement space, while the proper orthogonal values indicate the mean squared values of the data in each axis (Feeny and Kappagantu, 1998).

POD has been useful in uncovering spatial coherence in turbulence (Lumley, 1970; Lumley, 1967; Berkooz *et al.*, 1993) and structures (Cusumano and Bai, 1993; Cusumano *et al.*, 1993), determining the number of active state variables in a system (Berkooz *et al.*, 1993; Cusumano and Bai, 1993; Cusumano *et al.*, 1993), and in uncovering modal interactions (Davies and Moon, 1997). Proper orthogonal modes have been treated as empirical modal bases for discretizing nonlinear partial differential equations by Galerkin projections in turbulence applications (Berkooz *et al.*, 1993) and in structural dynamics (FitzSimons and Rui, 1993; Murphy, 1996; and Sipic *et al.*, 1996; Kappagantu, 1996; Azeez and Vakakis, 1997), and also for system identification (Yasuda and Kamiya, 1997; Lenaerts *et al.*, 2000).

Cusumano and Bai (1993) and Davies and Moon (1997) observed that the POMs in particular nonlinear structures resembled the normal modes of the linearized system. A recent analysis has shown the the POMs may indeed converge to linear normal modes in multimodal free responses of symmetric lumped-mass linear systems, but *only* if the mass matrix has the form $m\mathbf{I}$ (which can be achieved by a coordinate transformation if the mass distribution is known) and if the system is lightly damped (Feeny and Kappagantu, 1998). This

provides a fundamental tie between the statistically derived POMs and the geometrically based linear normal modes in certain discrete systems.

This paper extends the previous geometric interpretations of POMs in discrete systems to one-dimensional distributed-parameter systems, in the setting by which the continuous systems are sensed with a discrete number of sensors. That is, the discrete POD is applied to discretely sampled continuous systems, and interpretations are made regarding the continuous system. The principal thrust of this paper is in analytically relating the statistically based POMs to the geometry of normal modes, and accounting for the effect of discretization. We do this for multi-modal linear responses, and single-mode nonlinear responses.

2 DISTRIBUTED-PARAMETER LINEAR SYSTEMS

In this section, we provide an analysis that shows that under certain conditions, the statistically formulated POMs converge approximately to the discretized, geometrically based normal modes in continuous systems with discrete measurements. This extends a previous result relating the POMs to linear normal modes in lumped parameter systems (Feeny and Kappagantu, 1998).

2.1 Analysis of POD for Modal Responses

We illustrate the idea by considering a one-dimensional distributed-parameter system, such as a beam or string of length l . As with the discrete case, the scenario involves knowledge of the mass distribution. Suppose the model of the system is

$$m(x)\ddot{y} + L_1 y = 0, \tag{1}$$

where $y(x, t)$ is a displacement, the “dots” represent partial differentiation with respect to time, and L_1 is a self-adjoint linear operator. Letting $u = m^{1/2}(x)y$, the system can be rewritten as $\ddot{u} + m^{-1/2}(x)L_1 m^{-1/2}(x)u = 0$, or

$$\ddot{u} + L_2 u = 0. \tag{2}$$

L_2 is self-adjoint. For this system with its boundary conditions, separation of variables leads to eigenvalues and eigenfunctions $\phi_i(x)$ which can be normalized such that

$$\int_0^L \phi_i(x)\phi_j(x)dx = \delta_{ij}.$$

The absence of the mass in this integral is critical for the formulation below.

Assuming the displacement can be measured at discrete locations, whether by probes, accelerometers, or strain gages, the displacement $u(x, t)$ of the system is sampled at coordinates x_1, \dots, x_M . This leads to a set of measurements $\mathbf{u} = [u(x_1, t) \cdots u(x_M, t)]^T$. The displacement is approximated as a truncated series of linear normal modes, such that $u(x, t) \approx \sum_{i=1}^{\hat{M}} q_i(t) \phi_i(x) = \phi^T \mathbf{q}$, where $\phi = [\phi_1(x) \cdots \phi_{\hat{M}}(x)]^T$ is a vector of the modal functions that are kept, and $\mathbf{q}(t) = [q_1(t) \cdots q_{\hat{M}}(t)]^T$ is the vector of modal coordinates. We will take $\hat{M} = M$ in this discussion. We define a matrix $\Phi = [\mathbf{v}_1 \cdots \mathbf{v}_M] = [\phi(x_1) \cdots \phi(x_M)]^T$. Thus, the vectors $\mathbf{v}_i = [\phi_i(x_1) \cdots \phi_i(x_M)]^T$ are spatial discretizations of the mode shapes $\phi_i(x)$. Then

$$\mathbf{u} = \Phi \mathbf{q}(t)$$

relates the discrete displacements of the beam to the discretizations of the mode shapes.

The displacements are sampled at time t_1, \dots, t_N . We construct an $N \times M$ ensemble matrix $\mathbf{U} = [\mathbf{u}(t_1) \cdots \mathbf{u}(t_N)]^T = [\Phi \mathbf{q}(t_1) \cdots \Phi \mathbf{q}(t_N)]^T$, or

$$\mathbf{U} = (\Phi \mathbf{Q})^T,$$

where $\mathbf{Q} = [\mathbf{q}(t_1) \cdots \mathbf{q}(t_N)]$ is an $M \times N$ matrix. The correlation matrix can thus be built as $\mathbf{R} = \frac{1}{N} \mathbf{U}^T \mathbf{U} = \frac{1}{N} \Phi \mathbf{Q} \mathbf{Q}^T \Phi^T$.

We now check whether \mathbf{v}_j is an eigenvector of \mathbf{R} by examining $\mathbf{R} \mathbf{v}_j = \frac{1}{N} \Phi \mathbf{Q} \mathbf{Q}^T \Phi^T \mathbf{v}_j$. The quantity $\Phi^T \mathbf{v}_j$ has elements $\mathbf{v}_i^T \mathbf{v}_j$. We assume now that the spatial discretization is evenly spaced. Then, $\mathbf{v}_i^T \mathbf{v}_j = \sum_{k=1}^M \phi_i(x_k) \phi_j(x_k) \approx (1/h) \int_0^L \phi_i(x) \phi_j(x) dx$ by the rectangular rule, where h is the spacing of the spatial discretization. Thus we approximate $\mathbf{v}_i^T \mathbf{v}_j \approx (1/h) \delta_{ij}$. If this approximation is reasonable, then the quantity $\Phi^T \mathbf{v}_j \approx [0 \cdots 0, 1/h, 0 \cdots 0]^T = \mathbf{h}_j$ has elements of approximately zero, except the j th element which is approximately $1/h$. There will always be some error in this approximation, and we have not estimated this error on the modal vectors. However, the error associated with the rectangular integration representation of the underlying orthogonality integral is on the order of kh^2 , where k is proportional to a characteristic curvature in the integrand (Forsythe *et al.*, 1977). Then $\mathbf{R} \mathbf{v}_j = \frac{1}{N} \Phi \mathbf{Q} \mathbf{Q}^T \mathbf{h}_j$. The ij th elements of $\mathbf{Q} \mathbf{Q}^T$ are $\sum_{k=1}^N q_i(t_k) q_j(t_k)$. If the frequencies of oscillation of $q_i(t)$ and $q_j(t)$ are distinct, then

$$\lim_{N \rightarrow \infty} \frac{1}{N} \sum_{k=1}^N q_i(t_k) q_j(t_k) = 0, \quad i \neq j.$$

Thus,

$$\lim_{N \rightarrow \infty} \frac{1}{N} \mathbf{Q} \mathbf{Q}^T = \mathbf{D}$$

which is diagonal with elements $d_{ii} = \sum_{k=1}^N q_i(t_k)^2 / N$, which are the mean squared values of $q_i(t)$.

In such case, $\mathbf{R}\mathbf{v}_j \rightarrow \Phi\mathbf{D}\mathbf{h}_j = \Phi\mathbf{h}_j d_{jj} = \mathbf{v}_j d_{jj}/h$. So, for large N , with evenly spaced data and distinct modal frequencies, the POMs converge approximately to \mathbf{v}_j , which are the discretized linear modes. In other words the POMs converge to $\mathbf{v}_j + \mathbf{e}_j$ where \mathbf{e}_j is an error vector. Furthermore, the POVs converge to d_{jj}/h , which is proportional to the mean squared modal coordinate.

Thus, we have an analysis which ties the statistically formulated POMs to the discretization of the nonlinear normal modes for multi-modal free responses of undamped systems with known mass distributions.

The role of the mass distribution is critical. The modal functions of equation (1) are orthogonal with respect to the mass distribution (and the linear operator), and are not otherwise perpendicular to each other. We can expect that discretized modes are similarly not mutually perpendicular. The POMs, however, are orthogonal (i.e. perpendicular) to each other, since $\mathbf{R}^T = \mathbf{R}$. Thus, for general mass distributions, this means that the POMs cannot approximately coincide with the discretized linear normal modes. Formulating with respect to the mass, as in equation (2), allows us to make a connection between POMs and normal modes in multi-modal responses. The limitation, of course, is that the mass distribution must be known (or else be uniform). Enhanced development of POD may be necessary to overcome this limitation.

While the above discussion is for multi-modal motions, we end this section with a comment about single-mode responses. Motion consisting of a single normal mode traces a straight line in coordinate space. Trivially, the principal axis of the data will line up with the normal mode, yielding a POM that corresponds to the linear normal mode. This is independent of the spatial discretization and the knowledge of the mass distribution. Thus, for systems with arbitrary spatial discretizations or arbitrary or unknown mass distributions, the POD can be meaningful if a single mode is activated. Single modes may be resonated in lightly damped systems. Experience suggests that the dominant POM approximates the dominant normal mode. Steady-state forced responses also follow a straight line in coordinate space. If the response is resonant, the line, and hence the POM, will be close to the resonated mode.

2.2 Numerical Examples

We apply these ideas to the multi-modal free vibration of two simple systems, a cantilevered beam and a hinged-hinged beam, for which theoretical modes are readily available for comparison. For each numerical simulation, we choose a uniform mass per unit length of $m(x) = 1$, a stiffness of $EI = 1$, and a length of $L = 1$. The clamp is at $x = 0$.

For the numerical simulation of the cantilevered beam, the clamp is at $x = 0$. For

Table 1: Inner products times h between the first five discretized natural modes of the cantilever beam.

	\mathbf{v}_1	\mathbf{v}_2	\mathbf{v}_3	\mathbf{v}_4	\mathbf{v}_5
\mathbf{v}_1	1.2092	-0.2213	0.2411	0.0381	-0.0008
\mathbf{v}_2	-0.2213	1.2327	-0.2498	0.0209	-0.0384
\mathbf{v}_3	0.2411	-0.2498	1.2646	-0.0636	0.0712
\mathbf{v}_4	0.0381	0.0209	-0.0636	1.0249	-0.0330
\mathbf{v}_5	-0.0008	-0.0384	0.0712	-0.0330	1.0436

this case, the modal functions are $\cosh(\beta_i x) - \cos(\beta_i x) - \sigma_i(\sinh(\beta_i x) - \sin(\beta_i x))$, where the successive values of β_i are 1.8751, 4.6941, 7.8547, 10.9955, 14.1372, and $(2i - 1)\pi/2$ for $i > 5$, and the values of σ_i are 0.7341, 1.0185, 0.9992, and 1.0000 for $i > 3$ (Inman, 1994). The modal frequencies are $\omega_i = \beta_i^2 \sqrt{EI/m}$, and are incommensurate.

The beam is “sampled” at ten equally spaced locations from $x = 0.1$ to $x = 1$. The displacements are expanded in a truncated modal series consisting of the first ten modes. Vibrations are induced through the modal variables, such that $\mathbf{q}(0) = [2, 1, 0.5, 0.25, 0.12, 0.1, 0.05, 0.05, 0.05, 0.05]^T$ and $\dot{\mathbf{q}}(0) = \mathbf{0}$. The vibrations were sampled through four fundamental periods at an interval of $\Delta t = 0.0179$, resulting in 400 time samples.

The success depends on the rectangular-rule inner-product approximation. With the current discretization, the rectangular rule uses end values as opposed to midpoints. The discrete inner products times h of the first five discretized modal vectors are given in Table 1, from which the approximation of orthogonality can be judged.

Figure 1 shows the comparison between the first four discretized linear normal modes along with the POMs computed under the circumstances given. The norms of the errors between these first four sets of normalized modes are 0.0582, 0.2433, 0.3021, and 0.0881. The mean norm of the error between the ten computed modes is 0.1881. The visual comparison in the higher modes was better than the modes shown.

The quality of the results varies with the situation. A different set of initial conditions may give rise to better or worse POM approximations. Trouble is observed when the amplitudes of two or more modes are similar (Feeny and Kappagantu, 1998).

We have also applied the method to a hinged-hinged beam. In putting ten “sensors” on the beam away from the endpoints, the spacing was $h = 1/11$. Here, the modal functions are $\phi_i(x) = \sin(i\pi x)$. The inner product between the discretized modal vectors was, to at least four decimal points, $\mathbf{v}_i^T \mathbf{v}_j = \delta_{ij}/h$. The modal frequencies, $\omega_i = i^2\pi^2$, are distinct and

widely spaced.

Vibrations were induced through the modal variables; $\mathbf{q}(0) = [2, 1, 0.5, 0.25, 0.12, 0.1, 0.05, 0.05, 0.05, 0.05]^T$ and $\dot{\mathbf{q}}(0) = \mathbf{0}$ were the initial conditions. The vibrations were sampled through four fundamental periods at an interval of $\Delta t = 0.0179$, resulting in 400 time samples. Figure 2 shows the comparison between the first four sets of modes. The higher modes visually compared as well as those shown. The norms of the errors between these first four sets of modes are 0.0037, 0.0049, 0.0052 and 0.0055. The mean norm of the error between the ten computed modes is 0.0863.

3 SYNCHRONOUS NONLINEAR MODES

A nonlinear normal mode can be viewed as an invariant manifold in the state-space description of a system (Shaw and Pierre, 1993). Here, proper orthogonal decomposition is employed on measurements of the displacement coordinates, rather than measurements of full states.

In the case of a synchronous nonlinear normal modal response (“synchronous” meaning that the displacement coordinates reach their extrema simultaneously), the dominant POM can be interpreted as a the major principal axis of the data on the nonlinear normal mode at the given level of response. Since the principal axes optimize the distribution of data from the axes, the dominant POM can be considered as an optimal fit of the nonlinear normal mode (Feeny and Kappagantu, 1998). This interpretation is valid at the given level of response, and as the amplitude of the response changes, the path of the synchronous normal mode changes, as does its best fit.

If the motion is on a higher-dimensional invariant manifold, for example if more than one synchronous nonlinear modes are active, or if the nonlinear normal mode is not synchronous, then the POMs would again represent principal axes of the ellipsoid of inertia associated with the sampled data. However, the relationship between the POMs and the “best fit” of the nonlinear normal modes is obscured.

Observations indicate that this fitting of the nonlinear normal modes by the POMs may extend to multi-modal nonlinear modal responses (Ma *et al.*, 1998). However, since the paths of the modal response vary with response amplitude and with modal coupling, such interpretations must be sought with caution.

3.1 A Nonlinear Example

A numerical example involves a beam which is hinged-hinged and has a discrete cubic spring at its midpoint. The parameters are $m = EI = L = 1$. The nonlinear normal modes

of this system were analyzed by Boivin *et al.* (1995). The equation of motion of the beam is

$$m\ddot{u} + EIu'''' + u^3\delta(x - l) = 0, \quad (3)$$

where $u(x, t)$ is the deflection of the beam and δ is the Dirac delta function. The boundary conditions are $u(x, t) = u''(x, t) = 0$ at $x = 0$ and $x = L = 2l$. Equation (3) can be discretized using the assumed-modes method (Meirovitch, 1997). If the assumed modes are taken to be the linear natural modes, and u is expanded in a truncated modal series as $u(x, t) = \sum_{i=1}^N q_i(t)\phi_i(x)$, where $\phi_i(x) = \sin(i\pi x/L)$, the resulting discretized equations of motion are $\ddot{\mathbf{q}} + \mathbf{\Lambda}\mathbf{q} + \mathbf{f}(\mathbf{q}) = \mathbf{0}$, where $\mathbf{\Lambda}$ is a diagonal matrix of natural frequencies squared, and $\mathbf{f}(\mathbf{q})$ is a vector of nonlinear functions of \mathbf{q} , whose elements are $f_i = u(l)^3 \sin(i\pi/2)$.

The simulation consisted of the first ten modes. The initial conditions were $\mathbf{q}(0) = [4.0000, 0, 0.2244, 0, -0.2291, 0, 0.1023, 0, -0.0561, 0]^T$ and $\dot{\mathbf{q}}(0) = \mathbf{0}$. Only the symmetric modes were excited, so the numerical computation was actually done on the five odd modal displacements and velocities. The system of equations was integrated using a standard fifth-order Runge-Kutta algorithm. This vector of initial conditions very nearly excites only the first nonlinear normal mode. Three periods of motion in this nonlinear mode were sampled at a step size of $\Delta t = 0.0255$. The number of data was $N = 180$. The animated modal vibration is shown in Figure 3. The mode shape changes with the amplitude, and with its stage in the modal vibration.

The displacements along the beam were obtained from the truncated modal expansion, and evaluated at $M + 1$ evenly spaced locations along the beam. The extra “sensor” is false, in that there are still only M independent sensors. It was added so that the evenly spaced discretization included the midpoint of the beam. The resulting displacement histories were loaded into an ensemble matrix, and a correlation matrix \mathbf{R} was built. While the extra pseudo sensor leads to a singular correlation matrix and a zero POV, no information is lost, and the modal decomposition is expressed in terms of the $M + 1$ “sensors”. The three largest POVs were 46.9601, 0.1227, and 0.0003. Thus the dominant POM comprises about 99.8 % of the mean signal power. The two dominant POMs are plotted in Figure 4. The dominant POM of the discrete measurements qualitatively fits the animated synchronous motion. Figure 5 plots the displacement of the midpoint of the beam against the displacement at location $x = l/6$. Superposed on this plot is a projection of the dominant POM onto this coordinate space. The POM is aligned with the principal axis of minimum moment of inertia of the data. These figures suggest that the discrete measurements can be used to depict the continuous nonlinear modal behavior by means of POD.

Figure 6 plots four of the odd modal coordinates against the first modal coordinate. This plot shows how the participation of each linear mode changes during the first nonlinear modal vibration. Superposed on these plots are the projections of the first POM computed from an ensemble of modal displacements.

Note that the POMs *do not* represent linearized normal modes. If they did, then the POMs projected in Figure 6 would be horizontal lines, because the coordinates q are the modal coordinates of the linearized system. This brings out an important distinction that the dominant POM is a best fit of the synchronous normal mode, and not its linearization. Perhaps in this context we can apply the comment of Berkooz *et al.* (1993), that although POD is a linear process, it “may not do the physical violence of linearization methods.”

4 CONCLUSION

We have formulated some relationships between the proper orthogonal modes and modes of vibration of continuous systems.

The POMs approximate the discretized linear normal modes for free multi-modal motions of distributed systems if the discretization is evenly spaced. The quality of the approximation is partly dependent on how well the integral orthogonality property of the modal functions transfers to the discretized modal vectors, for which the inner product can be seen as proportional to a rectangular-rule integration. The mass distribution must be known to make these conclusions, and the problem must be formulated in displacement coordinates defined such that the associated mass distribution is uniform. For the case of a uni-modal motion, the dominant POM converges to the active linear natural mode regardless of the mass distribution or spatial discretization.

The results were tested on a cantilevered beam and a hinged-hinged beam. The cantilevered beam was more prone to error, probably because its modal discretization did not preserve orthogonality as well as that of the hinged-hinged beam.

We summarized the geometric meaning of POD and applied it to a synchronous nonlinear normal mode of a nonlinear beam. The dominant POM from discrete displacements of the beam qualitatively matched the animation of the synchronous modal motion.

In short, we have worked toward establishing a bridge between statistically derived POMs and the geometry of normal modes, for multi-modal responses of linear continuous systems with known mass distributions and evenly spaced measurement locations, and also for single mode nonlinear responses. This complements a recent tie made for lumped mass systems. The broad goal for linear analyses is to open the door for POD to be applied as a modal analysis tool. To make this goal a reality, developments are needed to overcome the discretization restrictions and the requirement for a known mass distribution.

ACKNOWLEDGEMENT

This work was supported by the National Science Foundation (CMS-9624347).

REFERENCES

- Azeez, M. F. A., and Vakakis, A. F., 1998, "Using Karhunen–Loève Decomposition to Analyze the Vibroimpact Response of a Rotor," *Seventh Conference on Nonlinear Vibrations, Stability, and Dynamics of Structures*, Blacksburg, VA.
- Berkooz, G., Holmes, P., and Lumley, J. L., 1993, "The Proper Orthogonal Decomposition in the Analysis of Turbulent Flows," *Annual Review of Fluid Mechanics*, Vol. 25, pp. 539-575.
- Boivin, N., Pierre, C., and Shaw, S. W., 1995, "Non-Linear Normal Modes, Invariance, and Modal Dynamics Approximations of Non-Linear Systems," *Nonlinear Dynamics*, Vol. 8, pp. 315-346.
- Cusumano, J. P., and Bai, B.-Y., 1993, "Period-Infinity Periodic Motions, Chaos, and Spatial Coherence in a 10 Degree of Freedom Impact Oscillator," *Chaos, Solitons, and Fractals*, Vol. 3, No. 5, pp. 515-535.
- Cusumano, J. P., Sharkady, M. T., and Kimble, B. W., 1993, "Spatial Coherence Measurements of a Chaotic Flexible-Beam Impact Oscillator," *Aerospace Structures: Nonlinear Dynamics and System Response*, ASME AD-Vol. 33, pp. 13-22.
- Davies, M. A., and Moon, F. C., 1997, "Solitons, Chaos, and Modal Interactions in Periodic Structures," *Nonlinear Dynamics: The Richard Rand 50th Anniversary Volume*, A. Guran, ed., World Scientific, Singapore, 119-143.
- Feeny, B. F., and Kappagantu, R., 1998, "On the Physical Interpretation of Proper Orthogonal Modes in Vibrations," *Journal of Sound and Vibration* **211** (4) 607-616.
- FitzSimons, P., and Rui, C., 1993, "Determining Low Dimensional Models of Distributed Systems," *Advances in Robust and Nonlinear Control Systems*, ASME DSC-Vol. 53, pp. 9-15.
- Forsythe, G. E., Malcolm, M. A., and Moler, C. B., 1977, *Computer Methods for Mathematical Computations*, Prentice Hall, Englewood Cliffs.
- Georgiou, I. T., and Schwartz, I. B., 1996, "A Proper Orthogonal Decomposition Approach to Coupled Mechanical Systems," *Nonlinear Dynamics and Controls*, ASME DE-Vol. 91, pp. 7-12.
- Kappagantu, R. V., and Feeny, B. F., 2000, "Part 2: Proper Orthogonal Modal Modeling of a Frictionally Excited Beam," *Nonlinear Dynamics*, to appear.
- Kreuzer, E., and Kust, O., 1996, "Proper Orthogonal Decomposition—an Efficient Means of Controlling Self-Excited Vibrations of Long Torsional Strings," *Nonlinear Dynamics and Controls*, ASME DE-Vol. 91, pp. 105-110.
- Lumley, J. L., 1967, "The Structure of Inhomogeneous Turbulent Flow," *Atmospheric Turbulence and Radio Wave Propagation*, A. M. Yaglom and V. I. Tatarski, eds., Nauka, Moscow, pp. 166-178.
- Lumley, J. L., 1970, *Stochastic Tools in Turbulence*, Academic Press, New York.
- Meirovitch, L., 1997, *Principles and Techniques of Vibrations*, Prentice Hall, Upper Sad-

dle River.

Ma, X., Azeez, M. A. F., and Vakakis, A. F., 1998, "Nonparametric Nonlinear System Identification of a Nonlinear Flexible System Using Proper Orthogonal Mode Decomposition," *Seventh Conference on Nonlinear Vibrations, Stability, and Dynamics of Structures*, Blacksburg, VA.

Murphy, K., 1996, "Using the Karhunen-Loève Decomposition to Examine Chaotic Snap-Through Oscillations of a Buckled Plate," *Sixth Conference on Nonlinear Vibrations, Stability, and Dynamics of Structures*, Blacksburg, VA.

Ravindra, B., 1999, "Comments on 'On the Physical Interpretation of Proper Orthogonal Modes in Vibrations'," *Journal of Sound and Vibration* **219** (1) 189-192.

Shaw, S. W., and Pierre, C., 1993, "Normal Modes for Non-Linear Vibratory Systems," *Journal of Sound and Vibration*, Vol. 164, No. 1, pp. 85-124.

Sipicic, S. R., Bengeudouar, A., and Pecore, A., 1996, "Karhunen-Loève Decomposition in Dynamical Modeling," *Sixth conference on Nonlinear Vibrations, Stability, and Dynamics of Structures*, Blacksburg, VA.

Yasuda, K., and Kamiya, K., 1997, "Experimental Identification Technique of Nonlinear Beams in Time Domain," *ASME Design Engineering Technical Conferences*, Sacramento, on CD-ROM.

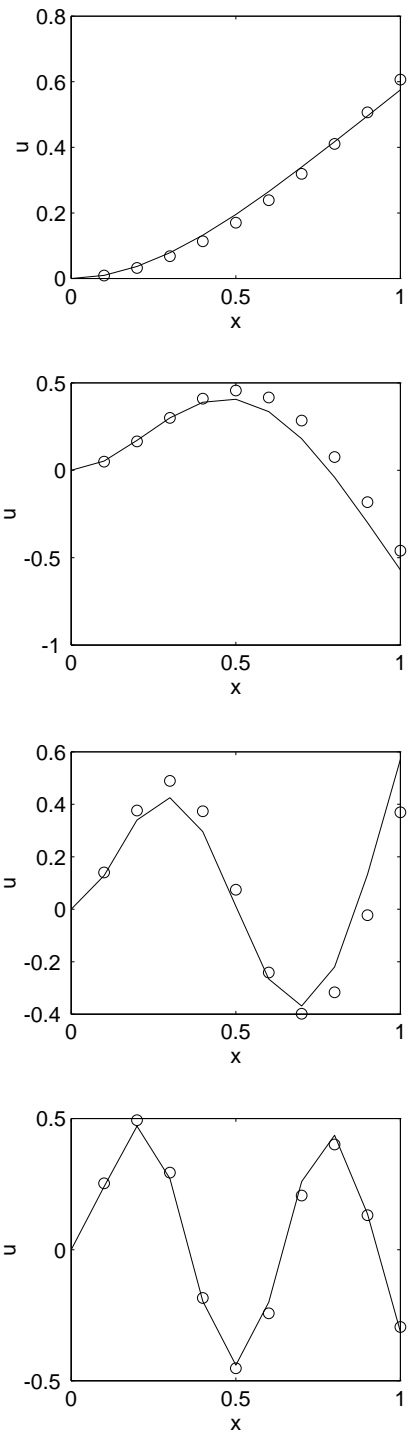


Figure 1: The first four discretized linear normal modes of a cantilevered beam are plotted with a solid line. The corresponding POMs are plotted with circles.

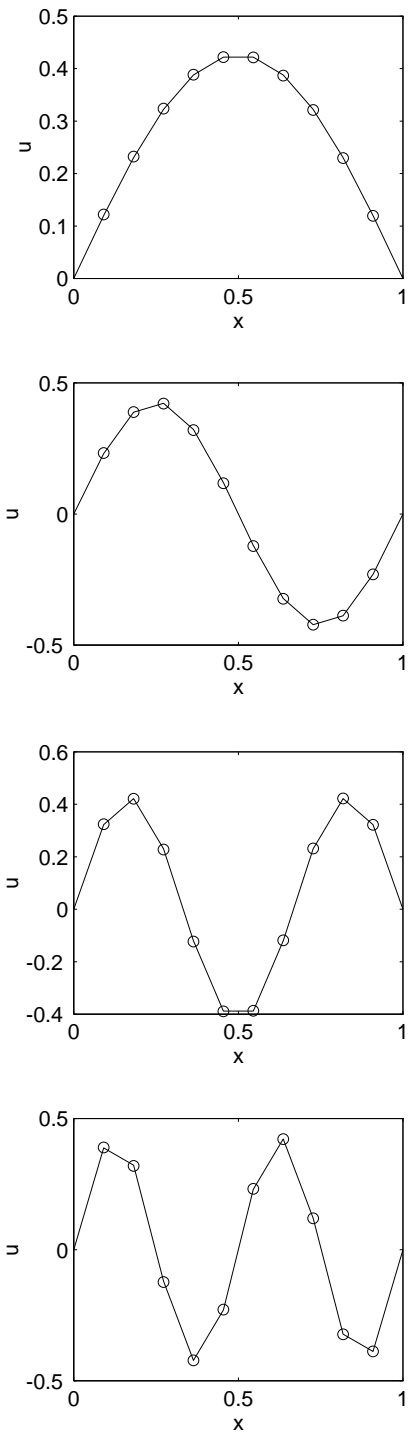


Figure 2: The first four discretized linear normal modes of a hinged-hinged beam are plotted with a solid line. The corresponding POMs are plotted with circles.

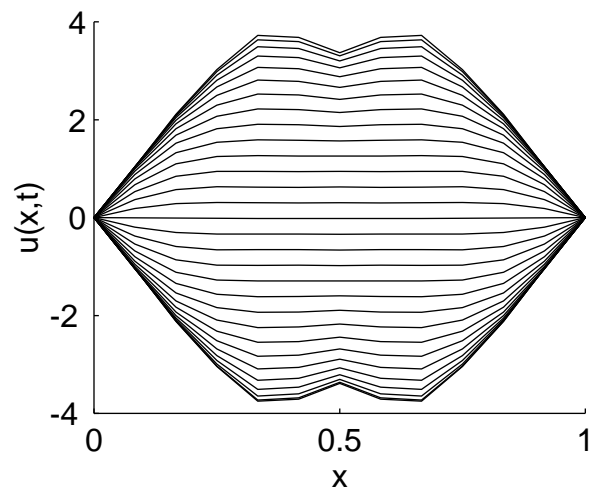


Figure 3: An animation of vibration in the first nonlinear normal mode of a nonlinear beam.

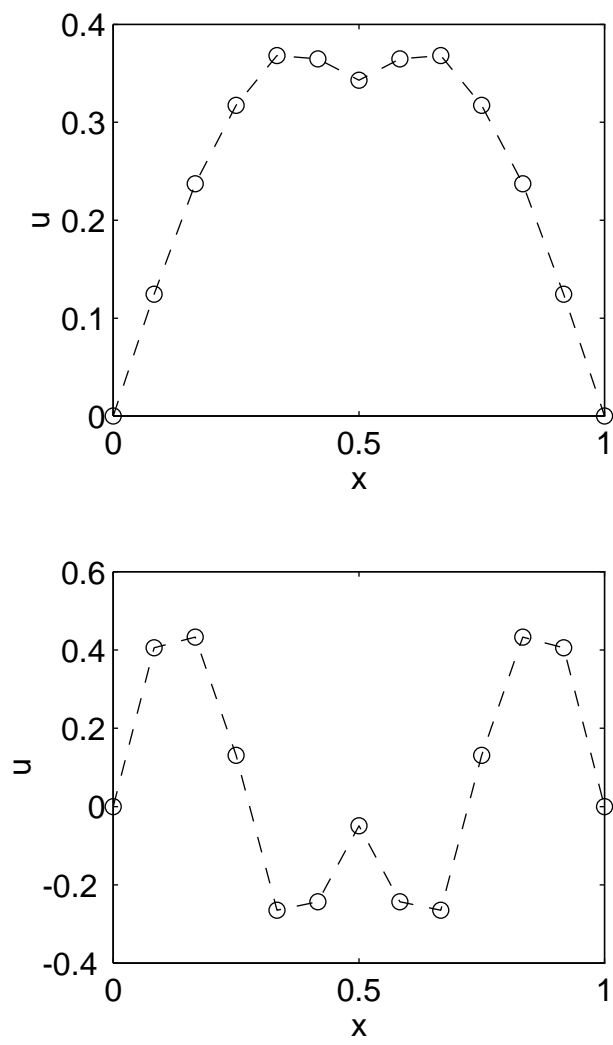


Figure 4: The two most dominant POMs for a nonlinear beam vibrating in the first nonlinear normal mode. The dominant POM corresponds to 99.8 % of the signal power.

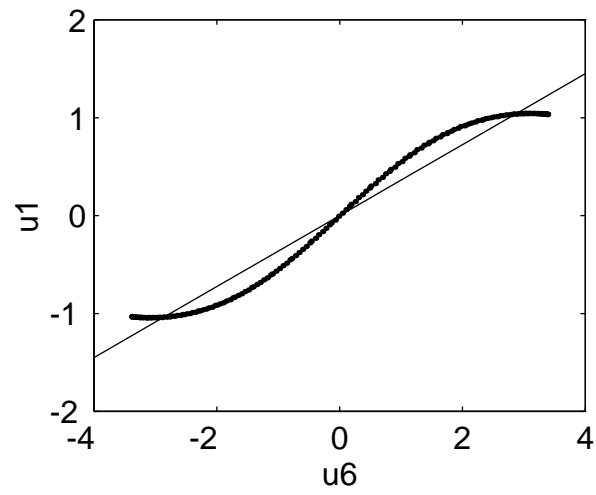


Figure 5: The deflection $u_1(t)$ at $x = 0.0825$ versus the deflection $u_6(t)$ at $x = 0.5$ during vibration in the first nonlinear normal mode. The straight line is the projection of the dominant POM.

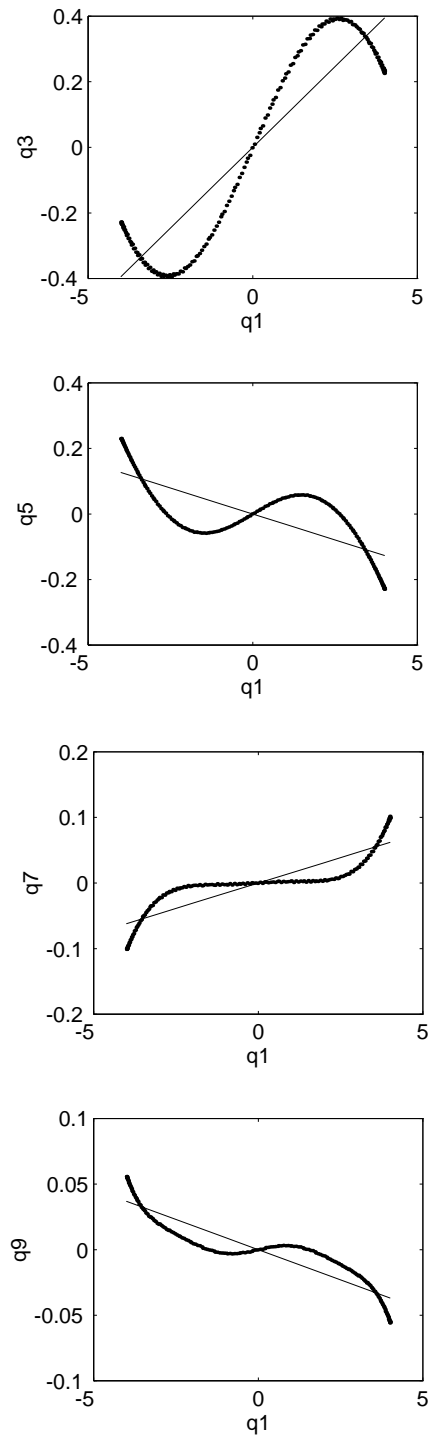


Figure 6: The deflections of the odd higher linear modal coordinates, q_3 , q_5 , q_7 , and q_9 , versus the first linear modal coordinate, q_1 , of a nonlinear beam during vibration in the first nonlinear normal mode. The straight lines are the projections of the dominant POM.